HHS Public Access

Author manuscript

Nat Struct Mol Biol. Author manuscript; available in PMC 2014 May 01.

Published in final edited form as:

Nat Struct Mol Biol. 2013 November ; 20(11): 1304–1309. doi:10.1038/nsmb.2692.

Mechanism of Allosteric Activation of SAMHD1 by dGTP

Xiaoyun Ji[1,6], **Ying Wu**[2,3,6], **Junpeng Yan**[4,6], **Jennifer Mehrens**[2,3], **Haitao Yang**[1,5], **Maria DeLucia**[2,3], **Caili Hao**[4], **Angela M. Gronenborn**[2,3], **Jacek Skowronski**[3,4], **Jinwoo Ahn**[2,3], and **Yong Xiong**[1]

[1]Department of Molecular Biophysics and Biochemistry, Yale University, New Haven, CT, USA

[2]Department of Structural Biology, University of Pittsburgh School of Medicine, Pittsburgh, PA, USA

[3]Pittsburgh Center for HIV Protein Interactions, University of Pittsburgh School of Medicine, Pittsburgh, PA, USA

[4]Department of Molecular Biology and Microbiology, Case Western Reserve School of Medicine, Cleveland, OH, USA

Abstract

SAMHD1, a deoxyribonucleoside triphosphate triphosphohydrolase (dNTPase), plays a key role in human innate immunity. It inhibits infection of blood cells by retroviruses, including HIV, and prevents the development of the autoinflammatory Aicardi-Goutières syndrome (AGS). The inactive apo-SAMHD1 interconverts between monomers and dimers, and in the presence of dGTP the protein assembles into catalytically active tetramers. Here, we present the crystal structure of the human tetrameric SAMHD1–dGTP complex. The structure reveals an elegant allosteric mechanism of activation via dGTP-induced tetramerization of two inactive dimers. Binding of dGTP to four allosteric sites promotes tetramerization and induces a conformational change in the substrate-binding pocket to yield the catalytically active enzyme. Structure-based biochemical and cell-based biological assays confirmed the proposed mechanism. The SAMHD1 tetramer structure provides the basis for a mechanistic understanding of its function in HIV restriction and the pathogenesis of AGS.

The sterile alpha motif and HD-domain containing protein 1 (SAMHD1) dNTPase plays dual roles in human innate immunity. It restricts HIV-1 infection in immune cells of myeloid

Correspondence should be addressed to J.A. (jahn@structbio.pitt.edu) or Y.X. (yong.xiong@yale.edu).
[5]Present address: School of Life Sciences, Tianjin University, Tianjin, China.
[6]These authors contributed equally to this work.

Author Contributions

X.J. performed protein crystallization, structure determination, and structure analysis; X.J. and H.Y. collected the diffraction data; Y.W., J.M., M.D. and J.A. performed the biochemical mutation experiments and data analysis *in vitro*; J.Y. and C.H. performed the cell-based experiments; J.A. provided experimental materials; X.J., Y.W., J.Y., H.Y., A.M.G., J.S., J.A., and Y.X. analyzed the data; X.J., Y.W., J.S., J.Y., J.A. and Y.X. designed the experiments; X.J., H.Y., A.M.G., J.S., J.A., and Y.X. wrote the manuscript.

Accession codes

The coordinates and structure factors have been deposited in PDB, with accession code 4BZC for the wild type and 4BZB for the RN mutant.

lineage and in quiescent CD4-positive T lymphocytes[1–5]. In these non-dividing cells, SAMHD1 reduces cellular dNTP levels to concentrations below the threshold required for reverse transcription of the viral RNA genome into DNA[6–8]. Furthermore, mutations in SAMHD1 are associated with an autoimmune condition, termed Aicardi Goutières Syndrome (AGS)[9,10], whose clinical manifestations resemble congenital viral infection[11,12]. AGS-associated SAMHD1 mutations appear to disrupt the dNTPase activity of SAMHD1. Thus, SAMHD1's ability to negatively regulate cellular dNTP levels is essential for its roles in innate immunity[13,14].

The dNTPase activity of SAMHD1 resides in its histidine-aspartate (HD) domain, with the N-terminal sterile alpha motif (SAM) domain involved in other activities[13–17]. A recent crystal structure of a dimeric SAMHD1 catalytic core fragment (SAMHD1c1, residues 120–626) suggested an allosteric, dGTP-stimulated mechanism for the promotion of the dNTPase activity of dimeric SAMHD1[14]. However, the SAMHD1c1 structure did not contain substrate or the dGTP cofactor, thus providing limited insight into the mechanism of SAMHD1 activation. Recent biochemical and functional studies revealed that SAMHD1 interconverts between an inactive monomeric or dimeric form and a dGTP-induced tetrameric form, which is the active dNTPase that restricts HIV[15,18].

To elucidate the mechanism of dGTP-induced oligomerization and allosteric activation of SAMHD1, we determined the crystal structure of the tetrameric SAMHD1–dGTP complex. The structure revealed two dGTP molecules in each of the four allosteric sites of the SAMHD1 tetramer. Comparison of the apo-SAMHD1 dimer with the SAMHD1–dGTP tetramer structures showed large, allosteric dGTP-induced conformational changes at the tetramer interfaces and the catalytic sites nearby, enabling the binding of the dNTP substrates. We validated the importance of the residues involved in these changes using biochemical and cell biological assays. Together, our results provide important mechanistic insights into dGTP-induced allosteric regulation of SAMHD1 catalytic function.

Results

To investigate the allosteric activation of SAMHD1 by dGTP, we determined the crystal structure of human SAMHD1 catalytic core (SAMHD1c2, residues 113–626) bound to dGTP (Fig. 1 and Table 1). SAMHD1c2 undergoes dGTP-dependent tetramerization and activation, similar to the full-length wild type protein[15]. To prevent substrate hydrolysis, we used the substrate analogue α-thio-dGTP (dGTPαS) to trap the complex in the substrate-bound conformation and determined the dGTPαS-SAMHD1c2 structure at 2.9 Å resolution. In addition, we solved the structure of a catalytically inactive mutant SAMHD1c2-RN (H206R D207N) with bound dGTP at 1.8 Å resolution. The two structures are virtually identical (RMSD 0.53 Å), except that the mutant complex does not contain the catalytic metal ion due to substitution of the conserved metal-coordinating residues His206 and Asp207 by Arg and Asn, respectively. For clarity, we refer to the structures as the dGTP–SAMHD1c2 complex when describing identical features in both structures. The overall structure comprises a well-defined catalytic core, with no density observed for only a short loop region (residues 278–283) and the C-terminus (residues 600–626).

The structure of the dGTP-induced SAMHD1 tetramer

One SAMHD1c2 tetramer of 222 point group symmetry (Fig. 1a,b; subunits labeled A, B, C and D) is in the asymmetric unit of the crystal. The AD and BC dimers are similar to the previously reported dimer structure of SAMHD1c1, burying 1750 $Å^2$ surface area per subunit at the dimer interface. These AD and BC interfaces are referred to as the dimer-1 interfaces in the following discussion. Two dimers associate further and form a very tight tetramer, resulting in a buried dimer-dimer interface of 4920 $Å^2$. The tetramerization is mainly mediated by the newly formed interfaces between A and C and between B and D. We refer to the AC and BD interfaces as the dimer-2 or tetramer interfaces. The subunits in the tetramer exhibit a virtually identical conformation, which is notably different from that in the dimeric SAMHD1c1 structure (Fig. 1c and Supplementary Fig. 1a). In particular, we observed a large conformational change at the new dimer-2 or tetramer interface (Fig. 1d). Tetramerization causes ordering of over 40 residues (residues 506–515, 531–547 and 584–599) that display clear density in the dGTP–SAMHD1c2 structure, whereas they were not observed in the previous SAMHD1c1 structure (Fig. 1b–d and Supplementary Fig. 1). These residues are critical for the formation of the SAMHD1 tetramer (discussed below).

The most striking feature in the SAMHD1c2 tetramer structure is the presence of 12 dGTP molecules. There are two dGTPs bound to each of the four allosteric sites and one dGTP bound to each of the four catalytic sites (Fig. 1b). Each allosteric dGTP-binding site is located at an interface of three subunits, highlighting the importance of dGTP for mediating the tetramer structure (Fig. 2a). This structural result agrees well with our solution biochemical data of dGTP-induced tetramerization[15]. Notably, residues 113–119 form a critical part of the allosteric dGTP-binding pocket (Figs. 1c and 2a), explaining why SAMHD1c1, which lacks these residues, only crystallized as a dimer[14].

dGTP–Mg^{2+}–dGTP binding at the allosteric site of SAMHD1

The allosteric dGTPs interact with an extensive network of hydrogen-bonding residues and exhibit excellent shape and size complementarity with the binding pocket at a three-subunit interface (Fig. 2a). Since all four allosteric dGTP-binding sites are identical, we selected the ACD interface to discuss these interactions. One of the two dGTPs (designated as dGTP-1) interacts with residues D137, Q142 and R145 of subunit D, forming five hydrogen-bonding interactions with the Watson-Crick and the Hoogstein (N7) sites of the guanine base. The second allosteric dGTP (designated as dGTP-2) interacts at the Watson-Crick base sites with residues N358 and D330 of subunit C. In addition, numerous residues from subunits A (V156, H376, K377, R451, K455), C (R333, R352, K354, K523), and D (K116, N119) provide additional hydrogen-bonding and stacking interactions with the base, sugar, and triphosphate moieties of the two allosteric dGTPs (Fig. 2b and Supplementary Fig. 2). Any other base in this pocket would result in fewer hydrogen bonds or steric hindrance in the binding site. This provides a clear structural rational for the inability of other dNTPs to activate SAMHD1[14]. The size of the dGTP-binding pocket provides a snug fit to the deoxyribose ring, leaving little room for the 2′-hydroxyl group of a ribose of GTP (Supplementary Fig. 3a).

The two allosteric dGTPs are juxtaposed with a Mg^{2+} ion bridging their phosphate groups in a dGTP–Mg^{2+}–dGTP configuration (Fig. 2a and Supplementary Fig. 3b) and four such dGTP pairs at the four allosteric sites interlock the subunits in the SAMHD1 tetramer. Each pair accounts for a buried surface of ~900 $Å^2$ between the dGTPs and the three associated polypeptide chains. The magnesium ion is coordinated by five oxygen atoms of the β-γ phosphate groups of two dGTP molecules and one ordered water molecule in an octahedral geometry (Supplementary Fig. 3b). The unique dGTP–Mg^{2+}–dGTP pairing noted here has not been previously observed in the oligomerization and allosteric activation of other HD domain-containing proteins[19–21].

Tetramerization causes conformational changes of SAMHD1

The dGTP-mediated tetramerization induces a large conformational change in SAMHD1 in regions at the tetramer interfaces when compared with the SAMHD1c1 dimer (Fig. 1c,d). Three layers of symmetrical protein contacts around a 2-fold symmetry axis are formed between the subunits at the dimer-2 interface (Fig. 2c). The first layer forms an S-shaped interlocking interface on the surface of the tetramer (Figs. 1a and 2d). This interface involves the C-terminal region of the protein (residues 454–599) with a loop-turn-loop structure (residues 506–515 and 531–547, disordered in SAMHD1c1) inserting into the concave surface of the 2-fold symmetrical related neighbor. This surface also contains another region at the C-terminus of the structure (residues 584–599) that is disordered in the SAMHD1c1 dimer. The second layer of interaction involves a long α-helix (residues 352–373) whose C-terminus is sandwiched between the catalytic site and the allosteric dGTP-2 (Fig. 2e). The orientation of this helix in the tetramer is different from that in the SAMHD1c1 dimer, most likely enabling pivotal interactions required for the activation of the enzyme (discussed below). The third layer of interaction resides in the center of the tetramer with a loop-helix region (residues 325–333) engaging in direct protein-protein contacts as well as contacts to dGTP-2 (Fig. 2f). This further demonstrates the critical role that dGTP plays in SAMHD1 tetramerization.

Phosphorylation of SAMHD1 residue T592 has been reported recently as a key regulator of its antiviral function[22,23]. The phosphorylation is catalyzed by the cell-cycle regulator cyclin A2/CDK1 upon recognition of the target motif (^{592}TPQK^{595}) on SAMHD1[22–24]. Our structure shows that T592 resides in the newly ordered C-terminal region whose structure is stabilized by tetramerization (Fig. 2d). The ^{592}TPQK^{595} motif is close to the tetramer interface and is solvent exposed (Supplementary Fig. 4). Modeling of a phosphate group onto T592 suggests that phosphorylation does not affect tetramerization or the folding of the protein. This is consistent with the finding that phosphorylation of T592 does not change the dNTPase activity of SAMHD1[22,23].

Tetramer-disrupting mutations abolish SAMHD1 function

We carried out mutagenesis studies to verify that the contacts with the allosteric dGTPs and the associated tetramerization are important. Residue changes such as R333A, D330A N358A, and R352A H376A K377A reduced dGTP-induced tetramerization and dNTPase activity *in vitro*, as well as dNTPase and antiviral activities *in vivo* (Fig. 3). The importance

of the dGTP-binding residue D137 is supported by a previous study, reporting that the D137A mutation abolished SAMHD1 catalytic activity and dGTP-dependent tetramerization[14,15]. Similarly, changing residues engaged in the interactions along the tetramer interfaces, such as D361R H364K and K534E V537D L540D, abolished tetramerization and impaired hydrolysis of dNTP *in vitro* (Fig. 3a,b). These mutants were also unable to restrict HIV-1 and deplete dNTP pools when expressed in cells (Fig. 3c,d).

Tetramerization of SAMHD1 activates the enzyme

In addition to the dGTP–Mg^{2+}–dGTP bound at the allosteric sites, one dGTP molecule is bound in the catalytic site of each SAMHD1c2 subunit (Fig. 4a). The substrate-binding pocket is located near the dimer-2 interface, with the interface α-helix (residues 352–373) (Fig. 2e) lining along one side of the pocket (Fig. 4a,b). The other side of the binding pocket is close to the dimer-1 interface observed previously[14] and contains the canonical His and Asp (HD) residues required for catalysis[21] (Fig. 4c). A catalytic metal ion is coordinated by the side chains of residues H167, H206, D207, D311, and the oxygen of the α-phosphate group of the substrate (Supplementary Fig. 5). Comparison of the current dGTP–SAMHD1c2 structure with that of a homologous protein, EF1143 from *Enterococcus faecalis* (PDB ID 3IRH)[19], suggests that H210, H233 and D218 are the catalytic residues (Supplementary Fig. 5). The extensive network of interactions within the snug binding pocket orients dGTP for catalysis (Supplementary Fig. 5). NTPs are excluded as substrates because the 2′-hydroxyl group of a ribose would clash with residues L150 and Y374 in the pocket. Notably, the extra space and lack of specific interactions at the base edge result in the ability of SAMHD1 to accommodate all four dNTPs as substrates (Supplementary Fig. 5).

The dGTP-induced tetramerization and conformational change alter the size and shape of the substrate-binding pocket in the inactive dimer to enable dNTP binding by SAMHD1 (Fig. 4c). When compared with SAMHD1c1, little change appears at the dimer-1 interface while large structural rearrangements occur at the dimer-2 interface in SAMHD1c2 (Figs. 4a and 1d). A more open pocket in the inactive dimer closes up upon tetramerization, enclosing the dNTP substrate (Fig. 4c). Specifically, the α-helix that is sandwiched between the catalytic site and the dimer-2 interface moves ~3 Å towards the substrate to allow residues R366, H370, and Y374 to engage in hydrogen-bonding and stacking interactions with the phosphate, the deoxyribose, and the base of the substrate, respectively. In addition, the disordered side chain of K312 in the SAMHD1c1 dimer structure becomes ordered by interaction with a loop region (residues 303–308), which together with Y315 and R366 contacts the γ phosphate group of dGTP (Fig. 4b). Mutation of these residues (K312A Y315A R366A or H370A Y374G) abolished the catalytic activity of SAMHD1 (Fig. 4d), presumably because they are important for binding and orienting the dGTP substrate for catalysis.

Discussion

SAMHD1 has been identified as an HIV restriction factor in non-dividing cells and the allosteric dGTP-mediated dNTPase activity is key to its antiviral function. However, the

mechanism of allosteric activation of SAMHD1 was unknown. In particular, how allosteric dGTP induces the tetramerization of SAMHD1 and subsequently enables substrate dNTP binding and catalysis remained mysterious. The work presented here establishes the structural and biochemical basis for the catalytic mechanism of SAMHD1 (Fig. 5): In the absence of the dGTP cofactor, SAMHD1 exists as an inactive monomer or dimer, in which the substrate-binding pocket is unable to bind dNTP[15,18]. Upon binding of dGTP–Mg^{2+}–dGTP at the allosteric sites, the catalytically inactive SAMHD1 dimers tetramerize, inducing a large conformational change at the tetramer interface. This conformational change is transferred to the catalytic sites nearby, resulting in a change of the size and shape of the substrate-binding pocket. It is possible that once activated, the SAMHD1 tetramer can perform multiple catalytic cycles that enables dNTP to bind in a catalytically productive conformation. without having to go through the dimer-tetramer transition and associated conformational changes in each cycle, as our previous biochemical data show that SAMHD1 tetramers are stable in the presence of dGTP[15].

The antiviral activity of SAMHD1 is down-regulated by phosphorylation at residue T592 by cyclin A2/CDK1 kinase, resulting in inhibition of HIV infection only in non-dividing cells such as quiescent $CD4^+$ cells, macrophages and dendritic cells[1–4]. Our structural result shows that the ^{592}TPQK^{595} motif is solvent-exposed on the protein surface and that is it unlikely that phosphorylation affects the active conformation of the enzyme. This is consistent with the observation that phosphorylation of SAMHD1 does not influence its dNTPase activity[22]. Besides the dNTPase activity, SAMHD1 has also been implicated in nucleic acid binding and exonuclease activity[16,25,26], allowing for the possibility that phosphorylation of T592 affects other activities of SAMHD1 required for retroviral restriction. Alternatively, T592 phosphorylation could modulate the interaction between SAMHD1 and an unknown cellular cofactor, which, in turn may influence the activities of SAMHD1. Further detailed studies are needed to elucidate the regulatory effect of SAMHD1 phosphorylation.

The loss-of-function mutations of SAMHD1 also lead to the autoinflammatory Aicardi–Goutieres syndrome (AGS)[10]. Previous studies revealed that some of the AGS-linked SAMHD1 mutations disrupt the catalytic site (R143H/C and G209S). Our current structure now illustrates how other mutations such as those residing at the allosteric dGTP-binding sites (R145Q, H123P, Δ120–123, and M385V) or at the tetramer interfaces (L369S) interfered with SAMHD1 function. Overall, our results provide compelling evidence for the biological relevance of the SAMHD1 tetramer and offer a biochemical and structural basis for understanding SAMHD1 functions in the pathogenesis of both HIV infection and AGS.

Our structural results provide not only important mechanistic insights into the regulation of SAMHD1, but also inform on the broad class of HD-domain containing allosteric phosphohydrolases that oligomerize and are activated upon NTP or dNTP binding[19,20,27–29]. For these HD enzymes, it has been an open question how ligand binding at an allosteric site induces their activation. Our current structure suggests an elegant general mechanism, namely, the creation of an active enzyme by dNTP or NTP-induced oligomerization and reshaping of the substrate-binding pocket adjacent to the newly formed molecular interface (Figs. 4c and 5).

Online Methods

N-terminal 6×His-tagged SAMHD1c2 and its mutants were expressed in *Escherichia coli* and purified using Ni-NTA affinity and size-exclusion chromatography as previously described[15]. SAMHD1c2 and α-thio-dGTP (or the RN mutant and dGTP) were co-crystallized using the microbatch under-oil method. Diffraction data were collected at the Advanced Photon Source beamline 24-ID and the National Synchrotron Light Source beamline X25. The structure was solved by molecular replacement using the coordinates of SAMHD1c1 (PDB ID 3U1N) as a search model. Diffraction data and refinement statistics are summarized in Table 1. Inhibition of HIV-1 infection by SAMHD1 and dATP pools in U937 cells, using HIV-1 RT-based single nucleotide incorporation assay, were quantified as described previously[15,31].

Protein expression and purification

The cDNAs encoding residues 1–626 and 113–626 of SAMHD1 were individually cloned into the pET28b expression vector (EMDBioscience) with a 6×His-tag at the N-terminus. Site-directed mutants of SAMHD1 were constructed by QuikChange mutagenesis (Agilent). All proteins were expressed and purified as described previously[15]. In brief, SAMHD1 proteins were expressed in *E. coli* Rosetta 2 (DE3) cells grown in Luria-Bertani medium at 250 rpm, 18 °C for 16h. The lysates were prepared by passing re-suspended cells through a microfluidizer. Proteins were purified by Ni-NTA affinity and size exclusion chromatography. The proteins were stored in a buffer containing 25 mM Tris-HCl, pH 7.5, 150 mM NaCl, 1 mM DTT, 10% glycerol, and 0.02% sodium azide.

Crystallization and data collection

The SAMHD1c2 mutant (H206R D207N, RN) in a solution containing 20 mM Tris-HCl, pH 7.8, 50 mM NaCl, 5 mM $MgCl_2$, 0.02% Azide, 2 mM DTT was mixed with 4 mM dGTP (final concentration) and incubated at 4 °C for 30 min before crystallization. Crystals were grown at 25 °C using the microbatch under-oil method[32] by mixing 1 μL protein (5 mg/ml) with 1 μL crystallization buffer (100 mM SPG (Qiagen), pH 7.4, 25% PEG 1500). Crystals were improved by streak seeding. Crystals were cryo-protected by the addition of 20% (v/v) ethylene glycol. Diffraction data were collected at the National Synchrotron Light Source beamline X25 (wavelength 1.100 Å and temperature 100 K). Wild type SAMHD1c2 was co-crystallized with 4mM alpha-thio-dGTP (ChemCyte Incorporated) with the crystallization buffer containing 100 mM Bis-Tris pH 6.7 and 25% (w/v) PEG1500. Crystals were cryo-protected by 25% (v/v) glycerol. Data were collected at Advanced Photon Source beamline 24-ID-C (wavelength 0.979 Å and temperature 100 K). The data statistics are summarized in Table 1.

Structure determination and refinement

The structures were solved by molecular replacement using the previously published coordinates of SAMHD1c1 (PDB ID 3U1N) as a search model. The program PHASER[33] was used for the molecular replacement search. Four molecules were identified in an asymmetric unit of the crystal. The initial model was auto-built by Buccaneer[34] and refined by iterative rounds of TLS and non-crystallographic symmetry (NCS)-restrained refinement

using Refmac5[35], followed by rebuilding manually using Coot[36]. The high-resolution SAMHD1c2-RN structure was used as a reference model during the refinement of the wild type structure. Refinement statistics are summarized in Table 1. The final models were validated by MolProbity[37]. The Φ, Ψ angels of 98.6% of residues of the RN structure and 98.8% of the wild type structure lie within favored regions of Ramachandran plot while those of all residues lie in the allowed regions.

Tetramer dissociation assays by analytical size exclusion chromatography

SAMHD1 proteins (0.5 μM) were pre-incubated with dGTP (40 μM) or without dGTP, and the mixtures (50 μL) were injected to an analytical gel filtration column (Superdex200, 10×300 mm) equilibrated with a buffer containing 20 mM Tris-HCl, pH 7.8, 50 mM NaCl, 10 μM dGTP, 5 mM $MgCl_2$, 5% glycerol at a flow rate of 0.5 mL/min. The elution profiles (fluorescence trace of excitation at 282 nm and emission at 313 nm) were recorded. The tetramer (%) was calculated by integrating the areas containing tetramer peak and monomer/dimer peak[15].

Deoxyribonucleoside triphosphate triphosphohydrolase (dNTPase) assays

Assays of SAMHD1 enzymatic activities were carried out in a reaction buffer containing 20 mM Tris-HCl, pH 7.8, 50 mM NaCl, 2 mM $MgCl_2$, 5% glycerol, 25 μM dGTP, 1 mM dATP, 5 μM BSA and 0.1 μM recombinant SAMHD1. The amounts of products were quantified by RP-HPLC after the reaction was quenched with 50 mM of EDTA after specific time intervals as describe previously[15]. The average rate of dA production (nmol/min mmol of SAMHD1) was calculated by performing linear regression analysis, after plotting the amount of dA product (on the ordinate) and the reaction time (on the abscissa).

Mammalian expression constructs and viruses

Human SAMHD1 deletion and point mutants were constructed using standard techniques and subcloned into the MSCV (puro) retroviral vector. VSV-G pseudotyped viral particles were produced from transiently transfected HEK 293T cells[15]. The single cycle HIV-1 luciferase reporter construct, constructed by N. Landau[38], was provided by Tom Hope and David McDonald.

SAMHD1 restriction assays

Wild type, or mutant FLAG epitope tagged SAMHD1 proteins were expressed in U937 cells (2×10^5 cells) by retroviral transduction. Two days post-infection, cells were selected by supplementing the medium with puromycin (2 μg/ml) and a day later plated in 24 well plates in the presence of 100 ng/ml phorbol 12-myristate 13-acetate (PMA) for 48 hours, kept for a day in fresh medium and then challenged with a single cycle HIV-1 NL4-3-Luc-R-E- expressing the luciferase reporter. Cell extracts were prepared from the infected cells 48 hours later and luciferase activity was quantified with the Luciferase Assay System (Promega). In dose response experiments cells were transduced with MSCV (puro) vectors expressing SAMHD1 at multiplicities of infection (moi) of approximately 1:1, 3:1, 10:1 and 30:1, followed by selection with puromycin. The increase in the SAMHD1 levels reflects

SAMHD1 expression from an increased number of integrated proviruses per cell. SAMHD1 levels in cell extracts were quantified by Western blotting.

Western Blotting

Cell extracts were separated by SDS-PAGE and transferred to a PVDF membrane for immunoblotting. SAMHD1 was detected with a monoclonal antibody specific for the FLAG-epitope tag (Sigma, F1804, 1:1000). α-tubulin used as a loading control was detected with an antibody purchased from Sigma-Aldrich (T5168, 1:5000). Immune complexes were revealed with fluorescent antibodies to mouse immunoglobulin G (LI-COR, 926-32210, 1:60,000) and quantified using an Odyssey Infrared Imager (Licor). In SAMHD1 dose response dNTPase and restriction assays, SAMHD1 fluorescent signals were normalized using those of α-tubulin as a reference.

Quantification of dATP pools in U937 cells

U937 cells were transduced with SAMHD1-expressing MSCV (puro) vectors as described above. dNTPs were extracted from PMA-differentiated U937 cells (5×10^5 cells), evaporated under vacuum at 70°C and the lyophilized extracts were stored in −80°C till the analysis. The dried material was re-suspended in 100 μL H_2O and dATP concentration was determined using HIV-1 RT-based single nucleotide incorporation assay, essentially as described previously[31]. Standard curves prepared with known amounts of dATP were used to calculate dATP amounts in test samples based on the extent of primer extension, as described previously[31].

Original images of blots used in this study can be found in Supplementary Figure 6.

Supplementary Material

Refer to Web version on PubMed Central for supplementary material.

Acknowledgments

We thank X. Jia, E. Weber, J. Fribourgh, H. Nguyen, and B. Summers for assistance and discussion, and Y. Zuo, Y. Li and C. Wang for technical assistance. We also thank the staff at the Advanced Photon Source beamline 24-ID and the National Synchrotron Light Source beamlines X25. This work was supported in part by funds from University of Pittsburgh School of Medicine (J.A.) and US National Institutes of Health grants AI097064 (Y.X.), AI100673 (J.S.), and P50GM82251 (A.M.G. and J.A.).

References

1. Descours B, et al. SAMHD1 restricts HIV-1 reverse transcription in quiescent CD4+ T-cells. Retrovirology. 2012; 9:87. [PubMed: 23092122]
2. Baldauf HM, et al. SAMHD1 restricts HIV-1 infection in resting CD4(+) T cells. Nat Med. 2012; 18:1682–9. [PubMed: 22972397]
3. Laguette N, et al. SAMHD1 is the dendritic- and myeloid-cell-specific HIV-1 restriction factor counteracted by Vpx. Nature. 2011; 474:654–7. [PubMed: 21613998]
4. Hrecka K, et al. Vpx relieves inhibition of HIV-1 infection of macrophages mediated by the SAMHD1 protein. Nature. 2011; 474:658–61. [PubMed: 21720370]
5. Berger A, et al. SAMHD1-deficient CD14+ cells from individuals with Aicardi-Goutieres syndrome are highly susceptible to HIV-1 infection. PLoS Pathog. 2011; 7:e1002425. [PubMed: 22174685]

6. St Gelais C, et al. SAMHD1 restricts HIV-1 infection in dendritic cells (DCs) by dNTP depletion, but its expression in DCs and primary CD4+ T-lymphocytes cannot be upregulated by interferons. Retrovirology. 2012; 9:105. [PubMed: 23231760]
7. Lahouassa H, et al. SAMHD1 restricts the replication of human immunodeficiency virus type 1 by depleting the intracellular pool of deoxynucleoside triphosphates. Nat Immunol. 2012; 13:223–8. [PubMed: 22327569]
8. Kim B, Nguyen LA, Daddacha W, Hollenbaugh JA. Tight interplay among SAMHD1 protein level, cellular dNTP levels, and HIV-1 proviral DNA synthesis kinetics in human primary monocyte-derived macrophages. J Biol Chem. 2012; 287:21570–4. [PubMed: 22589553]
9. Xin B, et al. Homozygous mutation in SAMHD1 gene causes cerebral vasculopathy and early onset stroke. Proc Natl Acad Sci U S A. 2011; 108:5372–7. [PubMed: 21402907]
10. Rice GI, et al. Mutations involved in Aicardi-Goutieres syndrome implicate SAMHD1 as regulator of the innate immune response. Nat Genet. 2009; 41:829–32. [PubMed: 19525956]
11. Crow YJ, Rehwinkel J. Aicardi-Goutieres syndrome and related phenotypes: linking nucleic acid metabolism with autoimmunity. Hum Mol Genet. 2009; 18:R130–6. [PubMed: 19808788]
12. Jepps H, Seal S, Hattingh L, Crow YJ. The neonatal form of Aicardi-Goutières syndrome masquerading as congenital infection. Early Hum Dev. 2008; 84:783–785. [PubMed: 18829186]
13. Powell RD, Holland PJ, Hollis T, Perrino FW. Aicardi-Goutieres syndrome gene and HIV-1 restriction factor SAMHD1 is a dGTP-regulated deoxynucleotide triphosphohydrolase. J Biol Chem. 2011; 286:43596–600. [PubMed: 22069334]
14. Goldstone DC, et al. HIV-1 restriction factor SAMHD1 is a deoxynucleoside triphosphate triphosphohydrolase. Nature. 2011; 480:379–82. [PubMed: 22056990]
15. Yan J, et al. Tetramerization of SAMHD1 Is Required for Biological Activity and Inhibition of HIV Infection. J Biol Chem. 2013; 288:10406–10417. [PubMed: 23426366]
16. White TE, et al. Contribution of SAM and HD domains to retroviral restriction mediated by human SAMHD1. Virology. 2012
17. Brandariz-Nunez A, et al. Role of SAMHD1 nuclear localization in restriction of HIV-1 and SIVmac. Retrovirology. 2012; 9:49. [PubMed: 22691373]
18. DeLucia M, Mehrens J, Wu Y, Ahn J. HIV-2 and SIVmac accessory virulence factor Vpx down-regulates SAMHD1 catalysis prior to proteasome-dependent degradation. J Biol Chem. 2013; 288:19116–19126. [PubMed: 23677995]
19. Vorontsov II, et al. Characterization of the Deoxynucleotide Triphosphate Triphosphohydrolase (dNTPase) Activity of the EF1143 Protein from Enterococcus faecalis and Crystal Structure of the Activator-Substrate Complex. J Biol Chem. 2011; 286:33158–33166. [PubMed: 21757692]
20. Oganesyan V, Adams PD, Jancarik J, Kim R, Kim SH. Structure of O67745_AQUAE, a hypothetical protein from Aquifex aeolicus. Acta Crystallogr Sect F Struct Biol Cryst Commun. 2007; 63:369–74.
21. Aravind L, Koonin EV. The HD domain defines a new superfamily of metal-dependent phosphohydrolases. Trends Biochem Sci. 1998; 23:469–472. [PubMed: 9868367]
22. White, Tommy E., et al. The Retroviral Restriction Ability of SAMHD1, but Not Its Deoxynucleotide Triphosphohydrolase Activity, Is Regulated by Phosphorylation. Cell Host Microbe. 2013; 13:441–451. [PubMed: 23601106]
23. Cribier A, Descours B, Valadão Ana Luiza C, Laguette N, Benkirane M. Phosphorylation of SAMHD1 by Cyclin A2/CDK1 Regulates Its Restriction Activity toward HIV-1. Cell Rep. 2013; 3:1036–1043. [PubMed: 23602554]
24. Errico A, Deshmukh K, Tanaka Y, Pozniakovsky A, Hunt T. Identification of substrates for cyclin dependent kinases. Adv Enzyme Regul. 2010; 50:375–99. [PubMed: 20045433]
25. Beloglazova N, et al. Nuclease Activity of the Human SAMHD1 Protein Implicated in the Aicardi-Goutieres Syndrome and HIV-1 Restriction. J Biol Chem. 2013
26. Goncalves A, et al. SAMHD1 is a nucleic-acid binding protein that is mislocalized due to aicardi-goutieres syndrome-associated mutations. Hum Mutat. 2012; 33:1116–22. [PubMed: 22461318]
27. Zimmerman MD, Proudfoot M, Yakunin A, Minor W. Structural Insight into the Mechanism of Substrate Specificity and Catalytic Activity of an HD-Domain Phosphohydrolase: The 5′-Deoxyribonucleotidase YfbR from Escherichia coli. J MolBiol. 2008; 378:215–226.

28. Kondo N, et al. Structure of dNTP-inducible dNTP triphosphohydrolase: insight into broad specificity for dNTPs and triphosphohydrolase-type hydrolysis. Acta Crystallogr D Biol Vrystallogr. 2007; 63:230–239.
29. Kondo N, Kuramitsu S, Masui R. Biochemica Characterization of TT1383 from Thermus thermophilus Identifies a Novel dNTP Triphosphohydrolase Activity Stimulated by dATP and dTTP. J Biochem. 2004; 136:221–231. [PubMed: 15496593]
30. Stuart DI, Levine M, Muirhead H, Stammers DK. Crystal structure of cat muscle pyruvate kinase at a resolution of 2.6 A. J Mol Biol. 1979; 134:109–42. [PubMed: 537059]
31. Diamond TL, et al. Macrophage Tropism of HIV-1 Depends on Efficient Cellular dNTP Utilization by Reverse Transcriptase. J Biol Chem. 2004; 279:51545–51553. [PubMed: 15452123]
32. Chayen NE, Shaw Stewart PD, Maeder DL, Blow DM. An automated system for micro-batch protein crystallization and screening. JAppl Crystallogr. 1990; 23:297–302.
33. McCoy AJ, et al. Phaser crystallographic software. J Appl Crystallogr. 2007; 40:658–674. [PubMed: 19461840]
34. Cowtan K. The Buccaneer software for automated model building. 1. Tracing protein chains. Acta Crystallogr D. 2006; 62:1002–1011. [PubMed: 16929101]
35. Vagin AA, et al. REFMAC5 dictionary: organization of prior chemical knowledge and guidelines for its use. Acta Crystallogr D Biol Crystallogr. 2004; 60:2184–95. [PubMed: 15572771]
36. Emsley P, Cowtan K. Coot: model-building tools for molecular graphics. Acta Crystallogr D Biol Crystallogr. 2004; 60:2126–32. [PubMed: 15572765]
37. Davis IW, et al. MolProbity: all-atom contacts and structure validation for proteins and nucleic acids. Nucleic Acids Res. 2007; 35:W375–83. [PubMed: 17452350]
38. Connor RI, Chen BK, Choe S, Landau NR. Vpr Is Required for Efficient Replication of Human Immunodeficiency Virus Type-1 in Mononuclear Phagocytes. Virology. 1995; 206:935–944. [PubMed: 7531918]

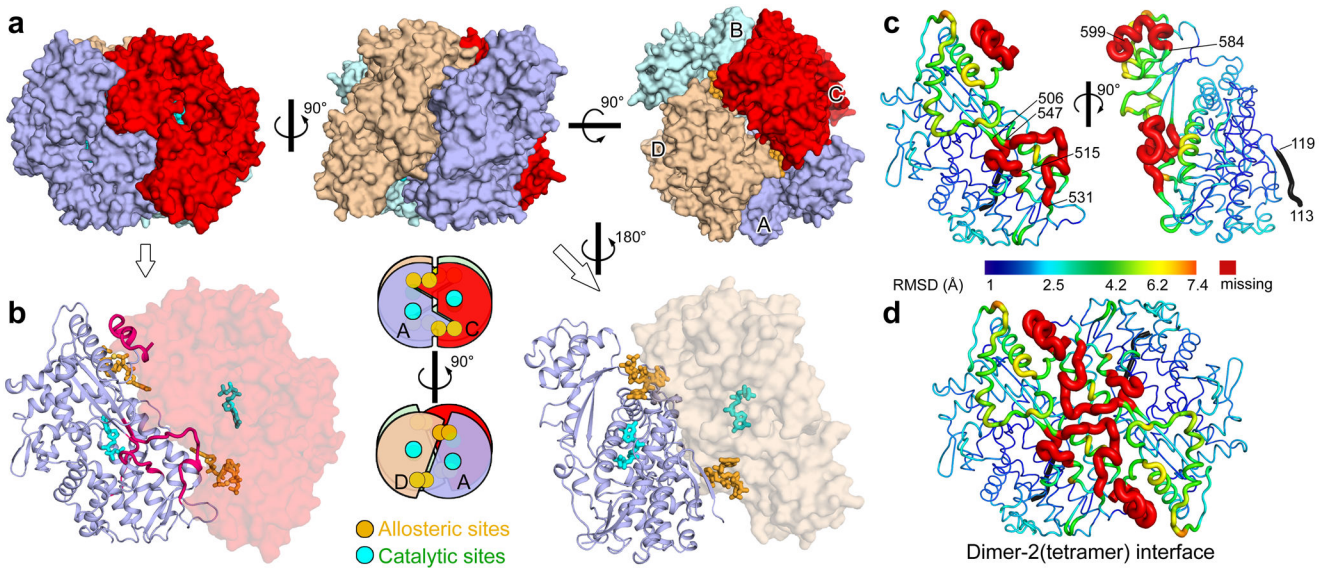

Figure 1. Crystal structure of the SAMHD1c2 tetramer in complex with dGTPs

(**a**) Surface representations of the tetramer in three orthogonal views. Subunits A, B, C and D are colored in light blue, pale cyan, red and wheat, respectively. (**b**) Left, the dimer-2 interface between subunits A (ribbon) and C (transparent surface). Regions that are disordered in the SAMHD1c1 structure are highlighted in magenta. Right, the previously observed dimer-1 interface between subunits A (ribbon) and D (transparent surface). Bound dGTP molecules are depicted in stick representations with the catalytic site dGTPs in cyan and the allosteric site dGTPs in orange. A schematic cartoon of the tetramer is provided in the middle box using the same color scheme as in the rest of the figure. (**c**) Putty representation of SAMHD1c2 subunit in two orthogonal views. The structure of SAMHD1c2 has been aligned to SAMHD1c1 using SHP[30]. The color spectrum and the coil thickness represent the deviation of the aligned Cα atoms (RMSD) in the two structures, which varies from 1 Å (blue) to 7.4 Å (orange). The disordered regions (residues 506–515, 531–547, 584–599, with each end labeled) in SAMHD1c1 are colored red and displayed with large thickness. Residues 113–119 which are not included in SAMHD1c1 are marked in black. (**d**) Dimer-2 (tetramer) interface with the most variable regions.

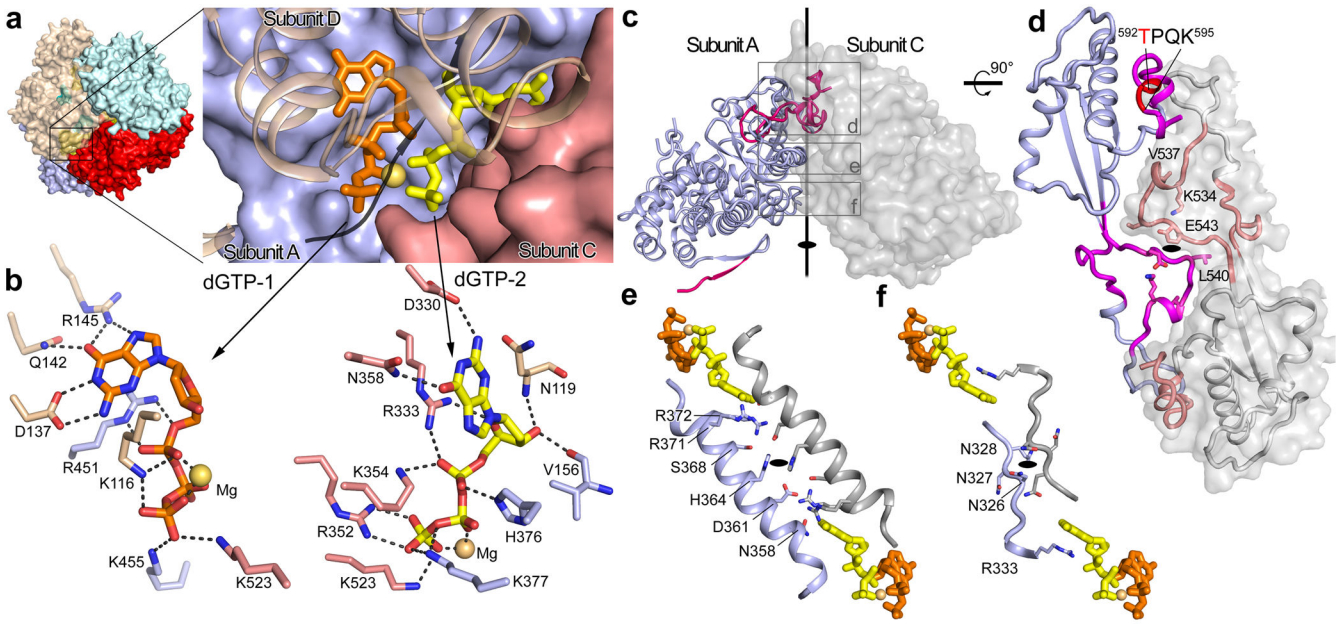

Figure 2. dGTP–Mg^{2+}–dGTP binding at the allosteric site induces tetramerization of SAMHD1

(**a**) Left, the SAMHD1c2 tetramer in surface representation, using the same color scheme as in Figure 1. Right, the allosteric dGTP binding site between subunits A, C, and D with the D subunit shown in semi-transparent ribbon representation to clearly illustrate the buried dGTP–Mg^{2+}–dGTP (yellow and orange sticks). The yellow sphere represents a magnesium ion. Residues 113–119 of subunit D are shown as a black ribbon. (**b**) Interactions between the two dGTP molecules and their surrounding residues. Residues are colored differently for each subunit, using the same color scheme as in Figure 1. Hydrogen bonds are shown as dashed lines. (**c**) The dimer-2 interface between subunits A (light blue ribbon) and C (grey surface). Residues that are not observed in the previous SAMHD1c1 dimer structure are highlighted in magenta. The three layers of interactions at the AC interface are boxed. The black oval and line indicate a 2-fold symmetry axis. (**b–d**) Details of the interactions in the three different layers, first (**b**), second (**c**), and third (**d**), respectively. Several key residues are shown in stick representation. The black oval in the center represents a two-fold axis perpendicular to the given view.

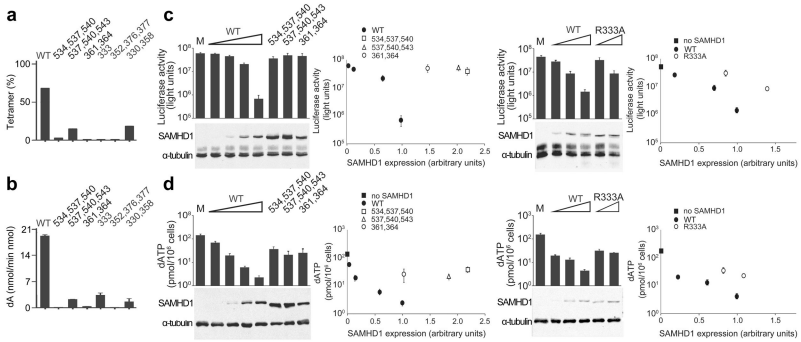

Figure 3. Mutagenesis of SAMHD1 residues involved in dGTP binding and tetramerization

(**a**) Quantification of SAMHD1 tetramer by analytical size exclusion chromatography[15], expressed as percentage of the total protein. The experiments were performed in duplicates and the average values are shown. (**b**) *in vitro* dNTPase assay of wild type (WT) and mutant SAMHD1 proteins. The nucleoside product (dA) was quantified by HPLC[15]. Each experiment was performed in triplicate. Error bars show the standard deviations (s. d.). (**c**) HIV-1 restriction and (**d**) intracellular dNTPase activities of WT SAMHD1, and the allosteric dGTP-binding site and the tetramer interface mutants. Luciferase activity in U937 cell extracts was quantified[15] and is shown in arbitrary units. dATP pools in U937 cells are presented in pmol/10^6 cells. WT and mutant SAMHD1 were detected by immunoblotting for the N-terminal epitope tag and α-tubulin was used as a loading control. U937 cells transduced with an empty MSCV (puro) vector (M) were used as a negative control. Luciferase reporter activity or dNTP levels in cells expressing WT or mutant SAMHD1 proteins are plotted as a function of protein expression levels, normalized to that of the highest expression level of WT SAMHD1. The values of luciferase activity and dATP amounts shown are averages of three replicates. Error bars, s. d.. Similar results were obtained in two independent experiments. Original images of blots used in this study can be found in Supplementary Figure 6.

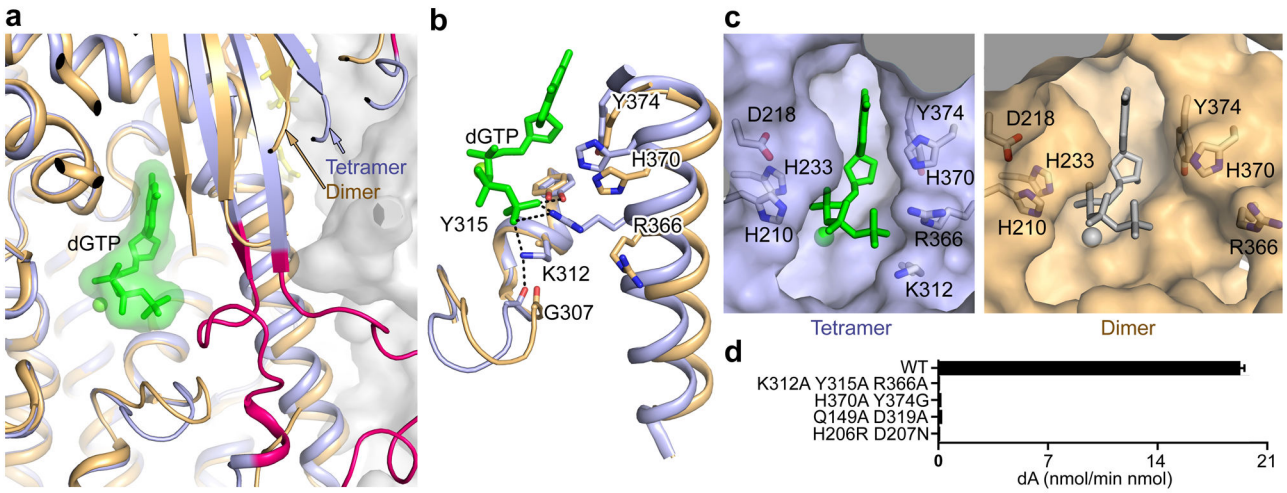

Figure 4. Comparison of SAMHD1c2 and SAMHD1c1 structures at the catalytic site

(**a**) Superposition of subunits of tetrameric SAMHD1c2 (light blue) and dimeric SAMHD1c1 (tan). Subunits A and C are shown in ribbon and surface representation, respectively. The dGTP substrate is depicted in green and the metal ion as a green sphere. Missing regions in SAMHD1c1 are highlighted in magenta in the SAMHD1c2 structure. (**b**) Conformational changes in the substrate binding pocket flanked by the α-helix at the dimer-2 interface. Key residues are shown in stick representation with hydrogen bonds shown as dotted lines. (**c**) Comparison of the substrate binding pockets (surface representation) in the two structures. The catalytic residues are shown on the left and key contact residues are shown on the right. The dGTP (grey) in the dimer is modeled based on the position in the tetramer. (**d**) dATPase assay for WT SAMHD1 and substrate binding site mutants. Each experiment was performed in triplicate. Error bars, s. d.

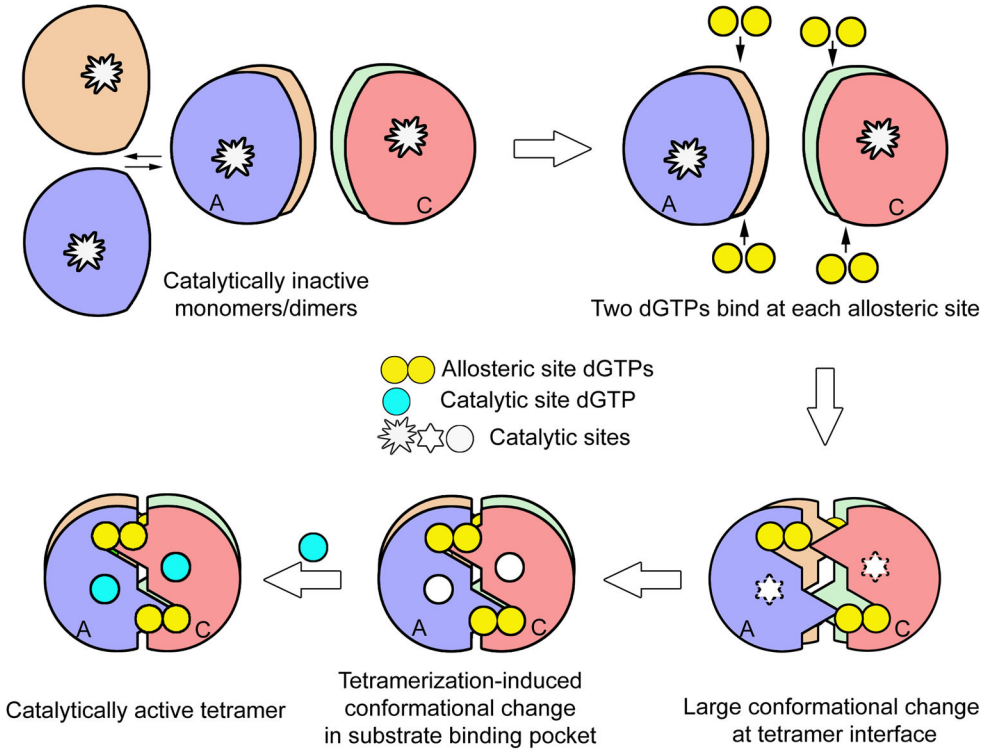

Figure 5. Schematic illustration of the mechanism of SAMHD1 activation by allosteric dGTP-induced tetramerization

Subunits of SAMHD1 are labeled A, B, C and D and the catalytically inactive monomer and dimers are shown with empty substrate binding pockets. Binding of four dGTP pairs at the allosteric sites promotes tetramerization and induces large conformational changes at the tetramer interface (AC and BD). This, in turn, causes conformational changes around the catalytic sites enabling dNTP substrate binding in a catalytically productive conformation.

Table 1

Data collection and refinement statistics

	H206R D207N SAMHD1c2 (residues 113–626)	Wild Type SAMHD1c2 (residues 113–626)
Data collection		
Space group	$P2_1$	$P2_1$
Cell dimensions		
a, *b*, *c* (Å)	87.20, 146.75, 98.72	79.00, 138.73, 93.72
α, *β*, *γ* (°)	90.00, 114.42, 90.00	90.00, 113.56, 90.00
Resolution (Å)	50.0–1.83 (1.86–1.83)*	50.0–2.88 (2.93–2.88)
R_{sym} or R_{merge}	0.103 (---**)	0.118 (0.895)
$I/\sigma I$	14.8 (1.0)	8.2 (1.2)
Completeness (%)	100 (100)	95.6 (97.4)
Redundancy	6.4 (5.2)	2.9 (3.0)
Refinement		
Resolution (Å)	48.7–1.83 (1.88–1.83)	49.7–2.88 (2.95–2.88)
No. reflections	177239	31009
R_{work}/R_{free}	0.188/0.206	0.190/0.245
No. atoms		
Protein	15950	15540
Ligand/ion	380	380
Water	877	34
B factors		
Protein	39.8	67.3
Ligand/ion	29.3	44.2
Water	40.5	36.0
r.m.s. deviations		
Bond lengths (Å)	0.005	0.012
Bond angles (°)	1.1	1.7

Two crystals for H206R D207N SAMHD1c2 structure and one crystal for Wild Type SAMHD1c2 structure were used for data collection and structure determination.

* Numbers in the brackets are for the highest resolution shell.

** R>=1